# Oxide dispersion strengthened magnesium: Effect of sonicated dispersion on the microstructure and mechanical properties

S. F. Hassan*

*Department of Mechanical Engineering, King Fahd University of Petroleum and Minerals,*
*P. O. Box 1061, Dhahran 31261, Saudi Arabia*

### Abstract

In this study, ultrafine (0.3 µm) aluminum oxide ($Al_2O_3$) particles were dispersed into commercially pure magnesium powder using the sonication method and processed by press-sinter-extrusion technique. The oxide particles dispersion in the processed magnesium microstructure was reasonably homogeneous and with good interfacial integrity. The dispersed oxide particles refined the grain morphology. They significantly improved the hardness, yield strength, tensile strength, ductility, and work-of-fracture of magnesium when added to a vol.% of up to 2.5. The dispersed oxide particles also changed the fracture mode of magnesium from brittle to ductile nature. However, the study also revealed that the ultrafine oxide particles dispersion was most effective in improving the overall mechanical properties of magnesium when added in an amount of 0.7 vol.%.

## 1. Introduction

The growing demand for energy-efficient equipment, conservation of rapidly depleting fossil fuel resources, and the protection of the deteriorating environment has brought attention to the lightweight materials, including magnesium as a structural material. Compared to the density of the existing structural metallic materials [1], the magnesium is thirty percent lighter than aluminum, sixty percent lighter than titanium, and seventy-five percent lighter than steel. Besides the lightweight, the magnesium has excellent castability, good damping capacity, and superior machinability. The magnesium has a long history of structural application [2, 3] and is expected to grow soon significantly. The supply of the magnesium metal is well secured by its abundant natural existence (sixth element in earth crust composition and third element in seawater composition) and the invention of the economically competitive extraction and refining process. Intensive research work is underway globally to improve the intrinsic limitations (i.e., relatively poor strength, ductility, corrosion resistance,

and thermal stability) of the magnesium and make it eligible to be a sustainable substitute of the existing structural metallic materials. Alloying with the compatible elements and/or reinforcing with the thermally stable stiffer second phase are considered to be the technically feasible ways to mitigate and/or circumvent these limitations. Between these two choices, the use of the second phase particles as reinforcement has reportedly been able to improve the mechanical properties of magnesium to the extent that it is beyond the limit of the traditional alloying process [4–11]. The shape, size, volume fraction, properties, and chemical compatibility of the second phase reinforcement dictate the extent of their effect on the resultant properties of the processed matrix material. Strengthening of metal by using harder second phase particles is maximized, with a trade-off in ductility, when they are well dispersed in the matrix in very small size and/or in relatively large volume fraction and effectively impede the dislocation motion [11, 12]. However, in the case of magnesium, it has been reported that the presence of extremely fine added second phase particles [6–11] induced metastable precipitation [13], and even the

---

*Corresponding author: tel.: +966 13 860 7787; fax: +966 13 860 2949, e-mail addresses: sfhassan@kfupm.edu.sa, itsforfida@gmail.com

grain refinement [14] can strengthen the matrix with simultaneous enhancement of its ductility, an anomalous to the generalized strength-ductility relationship. There is a compositional and/or processing limitation to produce favorable metastable precipitation, which does not exist in the case of the addition of external second phase particles. Added external second phase particles often introduce grain refinement and provide cumulative benefit to the metal matrix. Among all the added particle reinforcements, oxides, and, more specifically, the alumina ($Al_2O_3$) in a size range from nanometer to micrometer scale [7, 9, 10], reportedly was most compatible with magnesium to improve the structural properties. The alumina particles were reportedly dispersed in magnesium by using ingot and powder metallurgy processes. One of the earlier studies [10] revealed that the submicron-sized ($0.3\,\mu m$) ultrafine alumina provided the best combination of strength-ductility in magnesium when compared to the effect of nanometer and micrometer size particles. In this study, the ultrasonic method was used to disperse the different amounts of ultrafine ($0.3\,\mu m$) alumina particles in magnesium powder and investigated the effect of the added oxide dispersoids on the microstructure and mechanical properties of magnesium. Sonication was expected to disperse the ultrafine oxide particles efficiently and consequently maximize the exploitation of the oxide dispersion strengthening effect in magnesium.

## 2. Material and procedures

### 2.1. Material

High purity alpha alumina with an average size of $0.3\,\mu m$ (Baikowski, Japan) in three different vol.%, i.e., 0.7, 1.1, and 2.5 was dispersed in the commercially pure ($\geq 98.5\,\%$) magnesium powder (Merck, Germany) with a particle size range of $60$–$300\,\mu m$.

### 2.2. Processing

Oxide particles of the required vol.% were added to the magnesium powder in a glass beaker and dispersed using a probe sonicator (VC-50, Sonics) for ten minutes. Acetone was used as suspension media. The oxide dispersed magnesium suspension was kept in the oven at $50\,°C$ to evaporate the acetone and was subsequently compacted to cylindrical preforms ($40\,mm$ height with $35\,mm$ diameter) at a pressure of $450\,MPa$ using a uniaxial hydraulic press. The preforms were coated with colloidal graphite, wrapped in aluminum foil, and sintered for $2\,h$ at $500\,°C$ in a tube furnace under inert argon gas atmosphere. Sintered oxide dispersed magnesium preforms were hot extruded at $250\,°C$ to produce $8\,mm$ diameter rods,

using an extrusion ratio of $19.1:1$. Extrusion was conducted in a 150-ton uniaxial hydraulic press, and each of the preforms took one minute to be extruded. Colloidal graphite was used as a lubricant. The preforms were preheated for $90\,min$ in a constant temperature furnace at $300\,°C$ before the extrusion process. The synthesis of the monolithic magnesium without oxide particles was carried out using precisely similar steps.

### 2.3. Density measurement

Density ($\rho$) of the monolithic and oxide dispersion strengthened (ODS) magnesium was measured on polished extruded samples following Archimedes' principle [9]. Distilled water was used as the immersion fluid. A Mettler Toledo model AG285 Electronic balance, with an accuracy of $\pm\,0.0001\,g$, was used to weigh the samples in water and air media. Theoretical densities of ODS magnesium were predicted using Rule-of-Mixture with an assumption of a fully--dense microstructure free from any dispersoid-matrix interfacial reaction. Vol.% of porosity in the extruded materials was calculated from the difference between the theoretical and experimental density values.

### 2.4. Microstructural characterization

Microstructural characteristics of the monolithic and ODS magnesium were studied on metallographically prepared extruded samples to investigate the oxide particles dispersion pattern, oxide-magnesium interfacial characteristics, and effect of the oxide particles dispersion on the grain morphology of magnesium. Field Emission Scanning Electron Microscope (FESEM) Tescan Lyra-3 equipped with Energy Dispersive Spectroscopy (EDS) and Meji MX7100 optical microscope were used for the characterization process. The grain morphology was determined using Matlab based Line-cut image analysis software.

### 2.5. Mechanical characterization

The bulk and microhardness of the monolithic and the ODS magnesium were determined on polished extruded samples. Bulk hardness measurements were conducted using a Rockwell 15T superficial scale in universal Rockwell hardness testing machine following ASTM E18-17 standard. Vickers microhardness was measured using a load of 50 gf and dwell time of $15\,s$ on a Beuhler MMT-3 automatic digital microhardness tester in accordance with ASTM E384-17 standard.

Extension-to-failure tensile tests on the monolithic and ODS magnesium were carried out on an Instron 3367 machine following the ASTM E8M-16a standard. The tensile tests were conducted on smooth cylindrical specimens, which were machined from the extruded

Ta b l e 1. Results of density, porosity, and grain morphology characterization of ODS magnesium

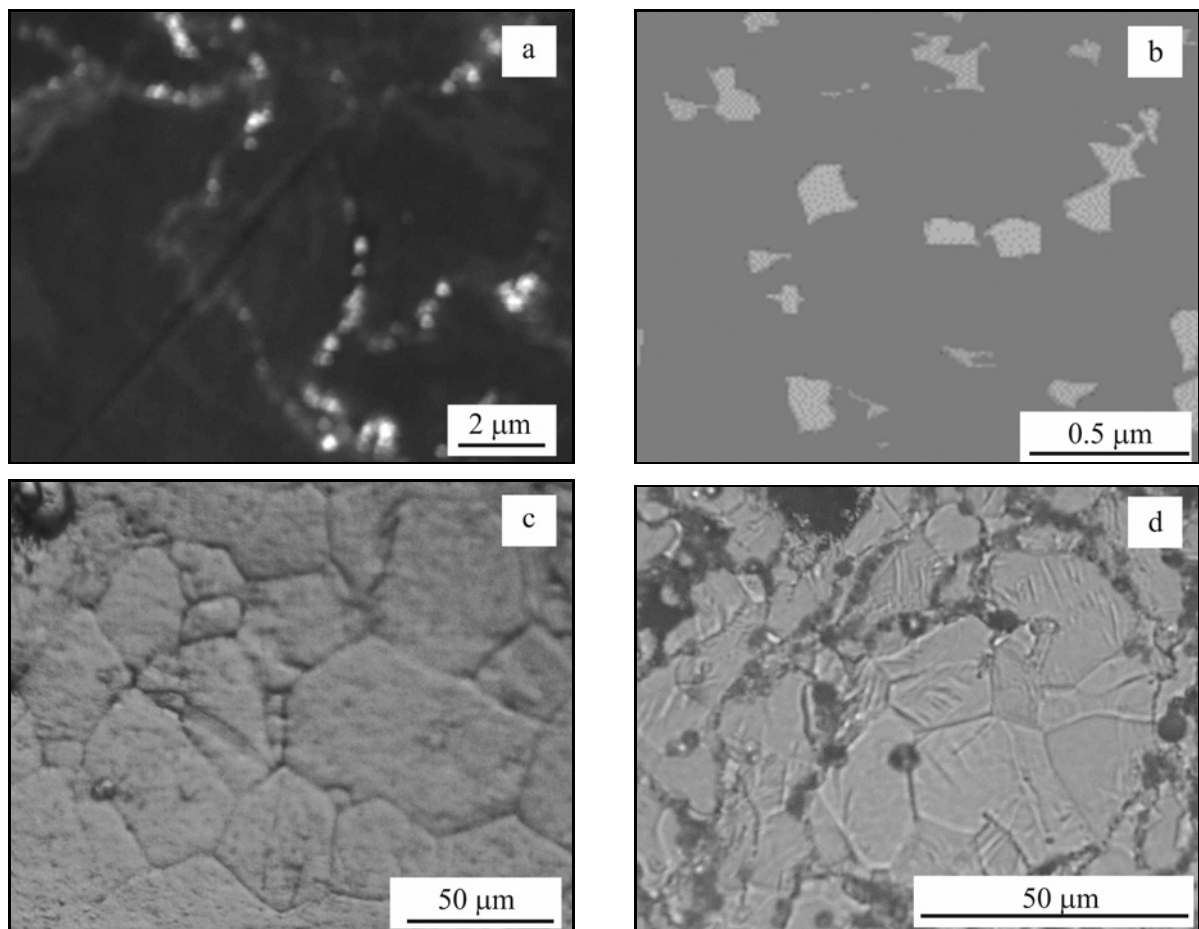| Materials | $Al_2O_3$ (wt.%) | Density (gm cm$^{-3}$) | | Porosity (%) | Grain morphology | |
|---|---|---|---|---|---|---|
| | | Theor. | Exp. | | size (µm) | Aspect ratio |
| $Mg/0.0Al_2O_3$ | 0.0 | 1.7400 | $1.7310 \pm 0.0149$ | 0.52 | $60 \pm 10$ | $1.6 \pm 0.3$ |
| $Mg/0.7Al_2O_3$ | 1.5 | 1.7548 | $1.7435 \pm 0.0140$ | 0.64 | $20 \pm 1$ | $1.3 \pm 0.6$ |
| $Mg/1.1Al_2O_3$ | 2.5 | 1.7647 | $1.7554 \pm 0.0064$ | 0.53 | $11 \pm 4$ | $1.7 \pm 0.5$ |
| $Mg/2.5Al_2O_3$ | 5.5 | 1.7954 | $1.7845 \pm 0.0289$ | 0.61 | $12 \pm 5$ | $1.7 \pm 0.7$ |
| $Mg/0.7Al_2O_3$ [7] | 1.5 | – | – | 0.27 | $63 \pm 16$ | $1.7 \pm 0.4$ |
| $Mg/1.1Al_2O_3$ [7] | 2.5 | – | – | 0.09 | $31 \pm 13$ | $2.2 \pm 1.3$ |



Fig. 1. Representative micrographs showing: 0.3 µm-$Al_2O_3$ particles distribution pattern and their interfacial integrity in $Mg/1.1Al_2O_3$ (using SEM & FESEM) in (a) & (b) and grain morphology for Mg and $Mg/0.7Al_2O_3$ in (c) & (d), respectively.

rod to a diameter of 5 mm and a gauge length of 25 mm. A constant crosshead speed of the machine was set at 0.254 mm min$^{-1}$ for all the samples. The stress-strain curves obtained from the tensile tests were used to compute the work of fracture (area under stress-strain curve) using excel software. Fractography of the tensile fractured samples was studied using the JEOL JSM-6460 LV scanning electron microscope to investigate the fracture mechanisms operative in the ODS magnesium under tensile loading.

## 3. Results

### 3.1. Synthesis and macrostructural characteristics

Meticulous physical observation of the compacted green and sintered preforms and the extruded rods of monolithic and ODS magnesium did not reveal the presence of any deformation or cracks or any other apparent defects.

T a b l e 2. Results of room temperature mechanical properties of ODS magnesium

| Materials | $Al_2O_3$ size (μm) | Hardness | | 0.2% YS (MPa) | UTS (MPa) | Ductility (%) |
|---|---|---|---|---|---|---|
| | | HR15T | HV | | | |
| $Mg/0.0Al_2O_3$ | | 43 ± 0 | 37 ± 0 | 111 ± 4 | 188 ± 5 | 7.3 ± 1.1 |
| $Mg/0.7Al_2O_3$ | | 49 ± 1 | 43 ± 0 | 209 ± 2 (88 %) | 256 ± 5 (36 %) | 12.4 ± 2.0 (70 %) |
| $Mg/1.1Al_2O_3$ | 0.3 | 56 ± 1 | 52 ± 0 | 182 ± 3 (64 %) | 237 ± 1 (26 %) | 12.1 ± 1.4 (66 %) |
| $Mg/2.5Al_2O_3$ | | 58 ± 0 | 53 ± 1 | 185 ± 2 (67 %) | 225 ± 3 (20 %) | 9.9 ± 0.6 (36 %) |
| $Mg/0.7Al_2O_3$ [7] | 0.05 | 56 ± 0 | 50 ± 1 | 191 ± 2 | 247 ± 2 | 8.8 ± 1.6 |
| $Mg/1.1Al_2O_3$ [7] | | 60 ± 1 | 70 ± 0 | 194 ± 5 | 250 ± 3 | 6.9 ± 1.0 |

Density and porosity measurement results for the extruded monolithic and ODS magnesium samples (see Table 1) revealed less than 1 % porosity, which indicated the dense material synthesis ability of the parameter used in the processing technique in this study.

### 3.2. Microstructural characteristics

Microstructural characterization revealed a necklace-type typical homogeneous distribution of the ultrafine oxide particles (see Fig. 1a) with apparent good interfacial integrity (see Fig. 1b). An increasing amount of oxide particle dispersions induced a significantly increasing grain refinement in the magnesium (see Figs. 1c,d and Table 1).

### 3.3. Mechanical characteristics

Mechanical characterization results showed (see Table 2) that the hardness (both bulk and micro) of magnesium was increased with the dispersion of the increasing amount of oxide particles used in this study.

The results of the room temperature elongation-to-failure tests (see Fig. 2 and Tables 2) revealed that sonication assisted dispersion of ultrafine oxide particles had significantly enhanced the strength, ductility, and limit of energy absorption capacity of the extruded magnesium. It also revealed that the tensile properties of magnesium reached to the highest level when dispersed with 0.7 vol.% of oxide particles and gradually decreased with further increment in the vol.% of oxide dispersions. Study of the tensile fracture surfaces revealed that the cleavage-steps representing the relatively brittle mode of fracture of magnesium (see Fig. 3a) transformed into pseudo-dimple (see Fig. 3b) and intergranular crack (see Fig. 3c) due to the presence of oxide particles dispersion, which was indicating the relatively ductile mode of fracture in ODS magnesium.
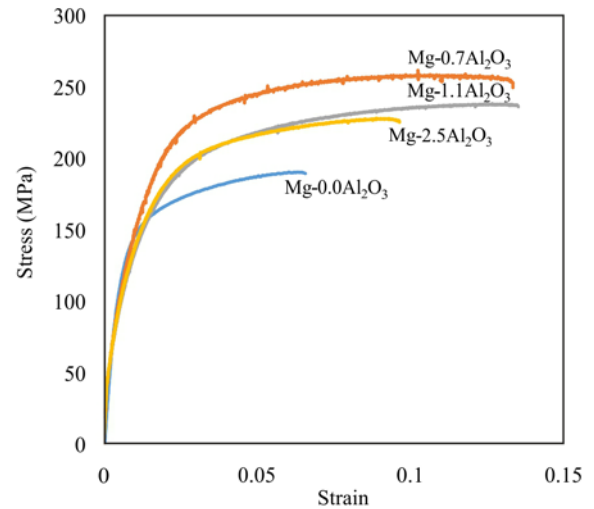


Fig. 2. Graph showing tensile stress-strain behavior of monolithic and alumina particles dispersed magnesium.

## 4. Discussion

### 4.1. Synthesis of reinforced and monolithic magnesium

Different vol.% of oxide particles were successfully well dispersed into magnesium using sonication [15, 16] and subsequent high extrusion ratio [4]. Finer ceramic particles typically agglomerate into clusters due to the presence of high surface energy induced strong van der Waals attractive forces among themselves. Sonication creates an alternating high and low--pressure waves in the liquid media leading to intense cavitation (i.e., the formation and immediate collapse of small vacuum bubbles) [17], which causes very high--speed impingement of the liquid media on the ceramic particles clusters [18] and deagglomerates them to distribute homogeneously in the space. The oxide ceramic reinforcement particles, along with the mag-
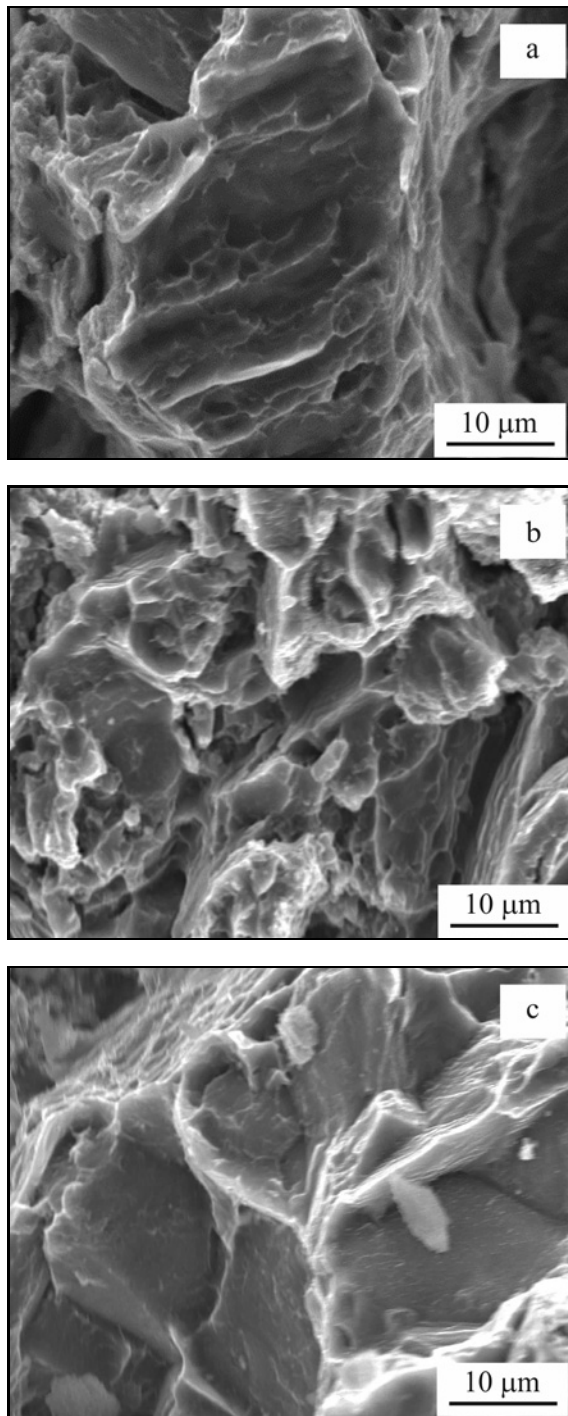
Fig. 3. Representative SEM fractographs showing: (a) brittle cleavage in monolithic magnesium, (b) pseudo-dimple, and (c) intergranular features in the case of 1.1 vol.% alumina particles dispersed magnesium.

nesium powders, were believed to be homogeneously suspended in the acetone media used in this study. Earlier researchers, who used sonication in powder metallurgy processing of aluminum and nickel-based metal matrix composite [19], also reported similar ob-

servations. It has to be noted that the sonication is effective in deagglomeration and subsequent homogeneous distribution of the fine reinforcement particles into liquid [17, 18, 20–22], semi-solid [23], and powder (in the colloidal state) [19] metal matrices.

No apparent physical defects, like deformation, oxidation, and/or surface cracks were visible in the compacted and sintered preform and extruded rods, which justified the appropriateness of the processing parameters. Achievement of the 99+% density in the monolithic and ODS magnesium (see Table 1) was believed to be the cumulative effect of the use of (a) broad range of the magnesium particles size (i.e., 60–300 μm), (b) very high compaction pressure (i.e., 450 MPa, which was much higher than the strength of magnesium and able to induce plastic flow to remove the interparticle micropores effectively and enhanced interparticles surface contact), (c) appropriate sintering parameters (i.e., $0.8\,T_{mp}$ (K) for 120 min), and (d) high extrusion ratio ($\sim 20$). It has to be noted that the high compaction pressure followed by reasonably high sintering temperature can synthesize magnesium with $> 96\,\%$ density when initial powder size is with 'very small size difference' [24] to $> 98\,\%$ density when initial powder size is with 'significantly large size difference' [25]. Subsequent hot extrusion with high extrusion ratio can further densify the magnesium to a near dense material [6, 7, 26].

### 4.2. Microstructural characteristics

Microstructural characteristics of the ODS magnesium with different vol.% of oxide particles are discussed here in terms of (a) oxide particles dispersion pattern, (b) oxide-magnesium interfacial characteristics, (c) effect of oxide particles dispersion on the magnesium grain morphology, and (d) porosity level in the magnesium microstructure.

Necklace-type distribution of sonication dispersed oxide particles in the ODS magnesium (see Fig. 1a) was observed in this study, and it is typical for externally added ultrafine second phase particles in the powder metallurgy processed metallic material [5, 15]. The tendency of externally added oxide particles agglomeration increased with an increase in their amount, and the apparent reason behind this could be the considerable differences between their initial particles (i.e., $Al_2O_3$ was 0.3 μm and Mg was 60–300 μm). Large size differences between the particles incline the smaller particles (oxide dispersions in this study) to fill the interstitial spaces between the large particles (magnesium powders in this study) during the drying and compaction stages. The high extrusion ratio in the subsequent thermomechanical processing was not effective enough to disperse the clustered interstitial oxide particles of the sintered preform. However, almost zero standard deviation in experimental den-

sity values (see Table 1) manifest the uniformity in the distribution pattern of oxide particles dispersions inside the ODS magnesium and justify the effectiveness of sonication induced mixing of the initial powders. Oxide-magnesium interfacial characteristics were found to be good (see Fig. 1b) as anticipated due to the aluminum-oxide/metal chemical compatibility [27] and were free from the presence of any visible debonding and/or microvoid.

The significant grain refinement in the processed ODS magnesium (see Figs. 1c,d and Table 1) was considered to be the cumulative effect of the ability of ultrafine oxide particles to nucleate new grains in the magnesium during the recrystallization stage and as well restrict the growth of recrystallized grains by boundary pinning [4, 15, 28] during the grain growth stage. However, the grain refinement ability of externally added oxide particles in magnesium was saturated at a level of their 1.1 vol.%, and further increment in their amount became ineffective to enhance the grain refining process proportionally. The limitation was seemingly due to the agglomeration tendency of oxide particles [28]. It should be noted that the grain refinement effect of the submicron size oxide dispersoid used in this study was more effective than that of nanometer size oxide dispersoid used earlier [7] (see Table 1).

Minimal porosity in the monolithic and ODS magnesium was corroborated by the experimental density values, as shown in Table 1. It could be attributed to the cumulative effect of enormous compaction pressure, appropriate sintering parameter, and high extrusion ratio used in this study.

### 4.3. Mechanical characteristics

The hardness of ODS magnesium experienced gradual increment (see Table 2) with the addition of an increasing amount of oxide particles. The increment in the hardness of magnesium can primarily be attributed to the increased resistance to the localized deformation during indentation process due to the presence of an increasing amount of stiffer aluminum oxide particles [4, 5] (elastic modulus is 390 GPa for $Al_2O_3$ and 45 GPa for Mg, [1]) and grain boundaries in the microstructure.

The results of the elongation-to-failure tensile test revealed a significant strengthening effect in terms of 0.2 % yield strength and ultimate tensile strength of magnesium (see Fig. 2 and Table 2) due to the addition of ultrafine oxide particles. The yield stress of a metallic material is the minimum level of stress required to initiate dislocation motion. It is governed by the dislocation density and magnitude of all the obstacles present in the microstructure to restrict the motion of dislocation under stress.

Synergic effect of the following strengthening mechanisms played a role in the enhancement of yield strength of metal with ultrafine oxide particles dispersoids in the microstructure:

(i) *Orowan strengthening mechanism* affects the strengthening of metal by dislocation – 'hard second phase' interaction and is effective when the dislocation encounters the hard second phase on the slip plane inside the grain. Contribution of this strengthening mechanism in powder metallurgy processed metal is expected to be insignificant [4–10] due to the fact the 'hard second phase' (oxide particles dispersion in this study) is mostly located at the grain and/or initial particle boundary.

(ii) *Hall-Petch strengthening mechanism* affects the strengthening of metal by dislocation – grain boundary interaction and can be predicted by Eq. (1):

$$\sigma^{\mathrm{HP}} = \sigma_{\mathrm{o}} + K/\sqrt{D}, \qquad (1)$$

where $\sigma_{\mathrm{o}}$ is friction stress, $K$ is stress direction-dependent constant, and $D$ is grain size. The Hall-Petch contribution is expected to be significant in the processed ODS magnesium due to the significant grain refinement [11, 12, 14].

(iii) *Increased dislocation density strengthening* affects the strengthening of metal by increasing the dislocation density, which was created due to the difference in elastic modulus (390 GPa for $Al_2O_3$ and 45 GPa for Mg [1]) and coefficient of thermal expansion ($7.6 \times 10^{-6}\,\mathrm{K}^{-1}$ for $Al_2O_3$ [1] and $27.045\,\mathrm{K}^{-1}$ for Mg [29]) between the metal and added second phase (fine aluminum oxide particles in this study). The contribution of increased dislocation density can be predicted by Eq. (2) [30, 31]:

$$\Delta\sigma = \sqrt{(\Delta\sigma_{\mathrm{EM}})^2 + (\Delta\sigma_{\mathrm{CTE}})^2}, \qquad (2)$$

where $\Delta\sigma$ represents an increase in the yield strength, $\Delta\sigma_{\mathrm{EM}}$ and $\Delta\sigma_{\mathrm{CTE}}$ are components of strength increment due to elastic modulus (EM) and coefficient of thermal expansion (CTE) mismatch. The components can be equated as:

$$\Delta\sigma_{\mathrm{EM}} = \sqrt{3}\alpha\mu_{\mathrm{m}}b\sqrt{\rho_{\mathrm{G}}^{\mathrm{EM}}} \qquad (3)$$

and

$$\Delta\sigma_{\mathrm{CTE}} = \sqrt{3}\beta\mu_{\mathrm{m}}b\sqrt{\rho_{\mathrm{G}}^{\mathrm{CTE}}}, \qquad (4)$$

where $\mu_{\mathrm{m}}$ is metal shear modulus, $b$ is Burgers vector, and $\alpha$ and $\beta$ are two coefficients for dislocation strengthening.

$\rho_{\mathrm{G}}^{\mathrm{EM}}$ is dislocation density from elastic modulus mismatch and equals to $4\gamma/b\lambda$ [32], where $\gamma$ is plastic shear, $b$ is Burgers vector, strain and $\lambda$ is local deformation field length related to the inter-particle dis-

T a b l e 3. Specific strength and work of fracture of ODS magnesium

| Materials | $Al_2O_3$ size ($\mu$m) | Work of fracture (J m$^{-3}$)* | $\sigma_{0.2\%YS}/\rho$ (kN/m kg$^{-1}$) | $\sigma_{UTS}/\rho$ (kN/m kg$^{-1}$) |
|---|---|---|---|---|
| $Mg/0.0Al_2O_3$ | | $12.0 \pm 1.1$ | 64 | 108 |
| $Mg/0.7Al_2O_3$ | | $28.2 \pm 4.9$ (135 %) | 119 (86 %) | 146 (35 %) |
| $Mg/1.1Al_2O_3$ | 0.3 | $25.0 \pm 3.3$ (108 %) | 103 (61 %) | 134 (24 %) |
| $Mg/2.5Al_2O_3$ | | $19.2 \pm 1.1$ (60 %) | 103 (61 %) | 126 (17 %) |
| $Mg/0.7Al_2O_3$ [7] | 0.05 | $19.9 \pm 3.9$ | 109 | 141 |
| $Mg/1.1Al_2O_3$ [7] | | $15.5 \pm 2.6$ | 110 | 142 |

*Determined from engineering stress-strain diagram using EXCEL software.

tance approximately equal to $r/(f)^{0.5}$ with dispersed oxide particle radius $r$ of $f$ (volume fraction).

$\rho_G^{CTE}$ is dislocation density from the coefficient of thermal expansion mismatch and equals to $A\varepsilon V_p/\{b(1-V_p)d\}$ [33], where $A$ is a geometric constant, $\varepsilon$ is thermal misfit strain between dispersed oxide particles and metal, $V_p$ is the volume fraction of dispersed oxide particle, $b$ is Burgers vector, and $d$ is the average diameter of dispersed oxide particles.

Apparently, the onset of yield strength led to the active dislocation-oxide particles interaction, resulted in the effective strain hardening (see Fig. 2) in the magnesium and increased the ultimate tensile strength. Despite yield strength and tensile strength of all of the ODS magnesium were significantly higher than those of the monolithic magnesium, the peak strength was achieved when the oxide particles dispersion was 0.7 vol.% and declined on the further addition in the vol.%. The strengthening effect of oxide particles dispersion was believed to be diminished due to their agglomeration in the microstructure. The overall strengthening effect (yield and tensile) of the 0.7 vol.% of submicron size oxide used in this study was found to be comparable (see Table 2) to the effect of 0.7–1.1 vol.% nanometer-sized dispersoid of the same oxide.

Tensile ductility of magnesium was significantly increased (see Fig. 2 and Table 2) when dispersed with oxide particles. Ultrafine oxide particles are known to be able to improve the ductility of hexagonal close-packed structured magnesium with a cumulative effect of their: (a) good dispersion [11], (b) grain refinement ability [14], and (c) possible ability in the activation of non-basal slip system [34]. Well dispersed thermally stable fine particles in the less ductile metal: (i) provide sites to open up the advancing cleavage crack front and dissipate the stress concentration, and (ii) alter the effective local state of stress from plane strain to one of plane stress in the neighborhood of the crack tip. Dislocation pile up at the grain boundary of fine-grained hexagonal close-packed structures induces intergranular crack propagation (see Fig. 3c) and enhances the ductility. However, the positive effect of the ultrafine oxide particles dispersion on the ductility of ODS magnesium was diminished with increasing vol.% and could be due to clustering in the microstructure. The work of fracture for a metal expresses its ability to absorb energy up to fracture under the applied tensile stress, computed using a stress-strain diagram, enhanced significantly (see Table 3) due to the dispersion of oxide particles following the same trend of ductility of the processed ODS magnesium. In essence, the sonicated dispersion of oxide particles made commercially pure magnesium eligible for both strength-based design (higher yield strength when compared to monolithic magnesium) and damage tolerant design (higher work of fracture when compared to monolithic magnesium). It has to be noted that the improvement of ductility and work of fracture of submicron size oxide dispersoid containing magnesium in this study was found to be significantly higher than the ductility and work of fracture of an equivalent amount of nanometer size oxide dispersoid containing magnesium reported earlier (see Tables 2, 3).

Tensile fracture surface analysis revealed that the typical cleavage steps representing brittle fracture [12] of magnesium (see Fig. 3a) were transformed into a mixed mode of fracture including (a) ductile fracture of pseudo-dimples [12] (see Fig. 3b) and (b) intergranular crack propagation (typical for hexagonal metal to improve its ductility [14]) (see Fig. 3c).

## 5. Conclusions

1. The sonication process was effective in the dispersion of ultrafine aluminum oxide particles in magnesium metal processed by powder metallurgy technique.

2. Homogeneous distribution of the oxide particles,

significant grain refinement, and presence of minimal porosity in the microstructure indicated the appropriateness of the sonication, compaction, sintering, and extrusion parameters used in this study.

3. Well-dispersed ultrafine oxide particles were effective in the improvement of hardness, yield strength, ultimate tensile strength, ductility, and work of fracture of commercially pure magnesium metal.

4. Ultrafine oxide particles effectively transformed the brittle mode of fracture in monolithic magnesium to ductile mode of fracture in ODS magnesium.

5. 0.7 vol.% of ultrafine aluminum oxide was found to be most effective in the improvement of the overall mechanical properties of magnesium.

## Acknowledgement

## References

[1] W. D. Callister Jr, D. G. Rethwisch, Materials Science and Engineering, ninth ed., John-Wiley & Sons, Inc., New York, 2007.

[2] M. Rashad, F. Pan, A. Tang, M. Asif, J. She, J. Gou, J. Mao, H. Hu, Development of magnesium-graphene nanoplatelets composite, J. Comp. Mater. 49 (2015) 285–293. doi:10.1177/0021998313518360

[3] Y. Ming, Y. Sirong, L. Enyang, L. Fanguo, Z. Yan, Z. Shanbao, L. Jingda, High-temperature damping capacity of fly ash cenosphere/AZ91D Mg alloy composites, Sci. Eng. Compos. Mater. 25 (2016) 197–204. doi:10.1515/secm-2016-0094

[4] S. F. Hassan, N. Al-Aqeeli, Z. M. Gasem, K. S. Tun, M. Gupta, Magnesium nanocomposite: increasing copperization effect on high temperature tensile properties, Powder Metall. 59 (2016) 66–72. doi:10.1080/00325899.2015.1109816

[5] J. Kubásek, D. Vojtěch, J. Maixner, D. Dvorský, The effect of hydroxyapatite reinforcement and preparation methods on the structure and mechanical properties of Mg-HA composites, Sci. Eng. Compos. Mater. 24 (2015) 297–307. doi:10.1515/secm-2015-0006

[6] S. F. Hassan, K. S. Tun, F. Patel, N. Al-Aqeeli, M. Gupta, Nickelization effect on the high temperature tensile properties of Mg-0.7Y$_2$O$_3$ nanocomposite, Arch. Metall. Mater. 63 (2018) 1411–1415. doi:10.24425/123819

[7] S. F. Hassan, M. Gupta, Development of high performance magnesium nano-composites using nano-Al$_2$O$_3$ as reinforcement, Mat. Sci. Eng. A-Struct. 392 (2005) 163–168. doi:10.1016/j.msea.2004.09.047

[8] B. Q. Han, D. C. Dunand, Microstructure and mechanical properties of magnesium containing high volume fractions of yttria dispersoids, Mat. Sci. Eng. A-Struct. 277 (2000) 297–304. doi:10.1016/S0921-5093(99)00074-X

[9] S. F. Hassan, M. Gupta, Effect of different types of nano-size oxide particulates on microstructural and mechanical properties of elemental Mg, J. Mater. Sci. 41 (2006) 2229–2236. doi:10.1007/s10853-006-7178-3

[10] S. F. Hassan, M. Gupta, Effect of particulate size of Al$_2$O$_3$ reinforcement on microstructure and mechanical behavior of solidification processed elemental Mg, J. Alloys Compd. 419 (2006) 84–90. doi:10.1016/j.jallcom.2005.10.005

[11] R. W. Cahn, Physical Metallurgy. North-Holland Publishing Company, Netherlands, 1970.

[12] D. R. Askeland, P. P. Fulay, W. J. Wright, The Science and Engineering of Materials. Cengage Learning, USA, 2011.

[13] A. Singh, M. Nakamura, M. Watanabe, A. Kato, A. P. Tsai, Quasicrystal strengthened Mg-Zn-Y alloys by extrusion, Scripta Mater. 49 (2003) 417–422. doi:10.1016/S1359-6462(03)00305-1

[14] Y. Wei, W. B. Lee, Mesoplasticity and its Applications, Materials Research and Engineering. Springer-Verlag, Berlin, 1993.

[15] S. Sankaranarayanan, R. K. Sabat, S. Jayalakshmi, S. Suwas, A. Almajid, M. Gupta, Mg/BN nanocomposites: Nano-BN addition for enhanced room temperature tensile and compressive response, J. Comp. Mater. 49 (2015) 3045–3055. doi:10.1177/0021998314559278

[16] B. A. Ahmed, A. S. Hakeem, T. Laoui, R. M. A. Khan, M. M. Al Malki, A. Ul-Hamid, F. A. Khalid, N. Bakhsh, Effect of precursor size on the structure and mechanical properties of calcium-stabilized sialon/cubic boron nitride nanocomposites, J. Alloys Compd. 728 (2017) 836–843. doi:10.1016/j.jallcom.2017.09.032

[17] O. Kudryashova, S. Vorozhtsov, On the mechanism of ultrasound-driven deagglomeration of nanoparticle agglomerates in aluminum melt, JOM 68 (2016) 1307–1311. doi:10.1007/s11837-016-1851-z

[18] Y. Yang, X. Li, Ultrasonic cavitation based nanomanufacturing of bulk aluminum matrix nanocomposites, J. Manuf. Sci. Eng. 129 (2007) 497–501. doi:10.1115/1.2714583

[19] S. Simões, F. Viana, M. A. L. Reis, M. F. Vieira, Aluminum and nickel matrix composites reinforced by CNTs: Dispersion/mixture by ultrasonication, Metals 7 (2017) art. no. 279. doi:10.3390/met7070279

[20] H. Dieringa, Processing of magnesium-based metal matrix nanocomposites by ultrasound-assisted particle dispersion: A review, Metals 8 (2018) art. no. 431. doi:10.3390/met8060431

[21] X. Y. Jia, S. Y. Liu, F. P. Gao, Q. Y. Zhang, W. Z. Li, Magnesium matrix nanocomposites fabricated by ultrasonic assisted casting, Int. J. Cast Metal. Res. 22 (2009) 196–199. doi:10.1179/136404609X367704

[22] Z. H. Wang, X. D. Wang, Y. X. Zhao, W. B. Du, SiC nanoparticles reinforced magnesium matrix composites fabricated by ultrasonic method, Trans. Nonferrous Metal. Soc. China 20 (2010) 1029–1032. doi:10.1016/S1003-6326(10)60625-5

[23] K. B. Nie, X. J. Wang, K. Wu, X. S. Hu, M. Y. Zheng, L. Xu, Microstructure and tensile properties of micro-SiC particles reinforced magnesium matrix composites produced by semi-solid stirring assisted ultrasonic vibration, Mat. Sci. Eng. A-Struct. 528 (2011) 8709–8714. doi:10.1016/j.msea.2011.08.035

[24] P. Burke, G. J. Kipouros, D. Fancelli, V. Laverdiere, Sintering fundamentals of magnesium powders, Canad. Metall. Quart. 48 (2009) 123–132. doi:10.1179/cmq.2009.48.2.123

[25] P. Burke, C. Petit, V. Vuaroqueaux, A. Doyle, G. J. Kipouros, Processing parameters and post--sintering operations effects in magnesium powder metallurgy, Canad. Metall. Quart. 50 (2011) 240–245. doi:10.1179/1879139511Y.0000000013

[26] I. A. Ibrahim, F. A. Mohamed, E. J. Lavernia, Particulate reinforced metal matrix composites – A review, J. Mater. Sci. 26 (1991) 1137–1156. doi:10.1007/BF00544448

[27] N. Eustathopoulos, M. G. Nicholas, B. Drevet, Wettability at High Temperatures, first ed., vol. 3, Pergamon Materials Series, Elsevier, UK, 1999.

[28] Y. C. Kang, S. L. Chan, Tensile properties of nanometric $Al_2O_3$ particulate-reinforced aluminum matrix composites, Mater. Chem. Phys. 85 (2004) 438–443. doi:10.1016/j.matchemphys.2004.02.002

[29] C. J. Smithells, Metals Reference Book. Butterworth--Heinemann Ltd, London, 1992.

[30] T. W. Clyne, P. J. Withers, An Introduction to Metal Matrix Composites. Cambridge University Press, New York, 1993.

[31] N. A. Fleck, G. M. Muller, M. F. Ashby, J. W. Hutchinson, Strain gradient plasticity: Theory and experiment, Acta Metall. Mater. 42 (1994) 475–487. doi:10.1016/0956-7151(94)90502-9

[32] N. Chawla, K. K. Chawla, Metal Matrix Composites. Springer Science + Business Media, Inc., New York, 2006.

[33] L. H. Dai, Z. Ling, Y. L. Bai, Size-dependent inelastic behavior of particle-reinforced metal-matrix composites, Compos. Sci. Technol. 61 (2001) 1057–1063. doi:10.1016/S0266-3538(00)00235-9

[34] C. S. Goh, J. Wei, L. C. Lee, M. Gupta, Ductility improvement and fatigue studies in Mg-CNT nanocomposites, Compos. Sci. Technol. 68 (2008) 1432–1439. doi:10.1016/j.compscitech.2007.10.057